Radiation and lifetimes of atoms inside dielectric particles

H. Chew*
Optical Sciences Division, Naval Research Laboratory, Washington, D.C. 20375
(Received 24 February 1988)

The transition rates of atoms inside spherical dielectric particles are computed and studied as functions of the transition frequency and of the physical properties of the host particle. The rates are found to range from about 0.2 to more than 1500 times the free-space value, depending on the location of the atom and other relevant physical parameters. The radiation from distributions of atoms inside liquid drops is also studied. Analytic and numerical results are given for the case of a uniform distribution of excited atoms. Large enhancements of the power output (some 100 times the value for the same distribution in bulk material) are found to occur under resonant conditions.

I. INTRODUCTION

There has recently been much interesting experimental work demonstrating that the lifetime of atoms in metallic cavities may be significantly different from the free-space values.[1-3] Similar changes in the lifetime have been found earlier for molecules near planar surfaces.[4,5] In the planar case it was found that a classical treatment, in which the atom or molecule is described as an oscillating electric dipole, gives results in excellent agreement with experiment.[5] It is therefore of interest to extend the classical treatment to atoms or molecules in or near small spherical particles[6,7] and compare the results with experiment. The spherical case is of special interest because an accurate theoretical treatment is possible, and liquid drops of almost perfectly spherical shape are easily produced experimentally. Moreover, there are numerous resonances associated with spherical particles, well known from elastic scattering, which are expected to have strong influences on the lifetimes of atoms nearby or inside.

In a recent paper,[7] the author derived analytic expressions for the transition rates of atoms or molecules inside and outside spherical dielectric particles. The results were derived on the basis of classical electromagnetic theory and were then shown to agree with those computed quantum mechanically with the linear-response formalism[8] adapted to spherical geometry.[7] Some numerical results, mostly for atoms outside the particle, were given in Ref. 7, in which it is found that the transition rates are oscillatory functions of the radial coordinate of the atom, and can be strongly enhanced when the transition frequency coincides with one of the resonance frequencies of the particle. In this paper we study the transition rates of atoms or molecules inside spherical dielectric particles in much greater detail, including quantitative discussions of the radiation due to a uniform distribution of excited molecules inside a liquid drop. The total power output due to this distribution is computed and found to be markedly different from the corresponding output due to the same distribution of molecules in the same bulk medium, especially for transition frequencies near resonances.

Section II presents numerical results on the transition rates of atoms inside nonmagnetic spherical dielectric particles in air as functions of radial coordinate, frequency, and the dielectric constant of the particle. The rates are normalized to the transition rates in the same medium in bulk in most cases, but comparison with free-space rates is also discussed. Very large enhancements of the transition rates, over 1000 times the free-space values, are found at certain resonances for size parameters $ka \sim 50$. These high rates depend sensitively on the size parameter and the refractive index of the particle, and somewhat less sensitively on the radial coordinate of the atom.

The total radiated power of a uniform population of excited atoms inside a spherical particle is computed in Sec. III. The results are normalized to the power due to the same population in bulk. Numerical results are given for radial and tangential polarizations, as well as the frequency dependence of the polarization averages. It is found that large resonance enhancements persists in spite of polarization and volume averaging.

II. TRANSITION RATES OF SINGLE ATOMS INSIDE A PARTICLE

Consider an atom at radial coordinates $\mathbf{r}'$ inside a spherical dielectric particle (medium 1) of radius a located in a dielectric medium (medium 2). It is shown in Ref. 7 that according to classical electromagnetic theory the rates for electric dipole transitions, normalized to the bulk value in medium 1, are given by

$$R^{\perp}/R_0^{\perp}=\frac{3\epsilon_1 n_1}{2\rho_1^2}\left[\frac{\epsilon_2}{\mu_2}\right]^{1/2}\sum_{n=1}^{\infty} n(n+1)(2n+1)\frac{j_n^2(y_1)}{y_1^2\,|D_n|^2} \tag{1}$$

for radial oscillations and

$$R^{\parallel}/R_0^{\parallel}=\frac{3\epsilon_1 n_1}{4\rho_1^2}\left[\frac{\epsilon_2}{\mu_2}\right]^{1/2}\times\sum_{n=1}^{\infty}(2n+1)\left[\left|\frac{[y_1 j_n(y_1)]'}{y_1 D_n}\right|^2+\frac{\mu_1\mu_2}{\epsilon_1\epsilon_2}\frac{j_n^2(y_1)}{|D_n'|^2}\right] \tag{2}$$

for tangential oscillations. The terms with the factor D_n are electric multipole (TM) terms and those with the factor D_n' are magnetic multiple (TE) terms. Here

$$n_1=\sqrt{\mu_1\epsilon_1},\ y_1=k_1r',\ \rho_{1,2}=k_{1,2}a,$$
$$D_n=\epsilon_1 j_n(\rho_1)[\rho_2 h_n^{(1)}(\rho_2)]'-\epsilon_2 h_n^{(1)}(\rho_2)[\rho_1 j_n(\rho_1)]' , \tag{3a}$$
$$D_n'=D_n \quad \text{with } \epsilon_\alpha\rightarrow\mu_\alpha,\ \alpha=1,2 . \tag{3b}$$

The denominators D_n and D_n' are the same as those of the elastic (Mie) scattering coefficients[9] and may become very small in magnitude when the transition frequency coincides with one of the natural (resonance) frequencies of the particle (the expansion coefficients for the internal fields also have the same denominators,[9] which is the origin of the "hot spots" inside particles illuminated by an electromagnetic wave[10]). For refractive indices up to about 1.5, the rates for both polarizations are smooth oscillatory functions of the radial distance r of the atom from the center for size parameter ka up to about 10. A higher refractive index tends to magnify the amplitudes of the oscillations. Increasing the size parameter leads to large resonances, and dramatic enhancements of the rates may occur, particularly near the surface. For refractive indices in the range 1.3–1.5, many large resonances are found for $ka\sim 50$ (these resonances are also reflected in the huge peaks in the internal fields; see, for example, the last two papers quoted in Ref. 10). A further increase in ka leads to wrinkly rate curves (as functions of r) with narrower and closer peaks, which can become very large near the surface at resonances.

These effects are illustrated in Figs. 1–8, which show the normalized transition rates for both radial and tangential polarizations of the radial coordinate of the molecule inside a dielectric sphere of radius a in air ($\mu_1=\mu_2=\epsilon_2=1$). These rates have been normalized to the rates of atoms in bulk medium 1 in order to isolate the effects of the particle versus those of the bulk medium. To compare the transition rates of atoms in the particle with the free-space rates, we need only to multiply the right-hand side of Eqs. (1) and (2) and the normalized rates in all the figures by $\sqrt{\epsilon_1}$, i.e.,

$$R^{\perp}/R^{\perp}_{\text{air}}=(R^{\perp}/R^{\perp}_0)(R^{\perp}_0/R_{\text{air}})$$
$$=(\mu_1^3\epsilon_1/\mu_2^3\epsilon_2)^{1/2}(R^{\perp}/R^{\perp}_0)=(R^{\perp}/R^{\perp}_0)\sqrt{\epsilon_1} ,$$

and similarly

$$R^{\parallel}/R^{\parallel}_{\text{air}}=(R^{\parallel}/R^{\parallel}_{\text{air}})\sqrt{\epsilon_1} .$$

This was done in Figs. 6 and 7; all the other figures show rates normalized to bulk values for medium 1. In these figures (1–8) the solid curves (scale on the left) are transition rates for radial oscillations and the dashed curves (scale on the right) are rates for tangential oscillations. Figure 1 shows the rates for molecules inside a glycerol drop ($\epsilon_1=2.1609$) with size parameter $ka=5$. Figures 2–8 show the rates for molecules inside a water drop ($\epsilon_1=1.7689$) in air. In Fig. 2, the rates are dominated by a resonance in the $n=58$ electric multipole ($E58$) term at

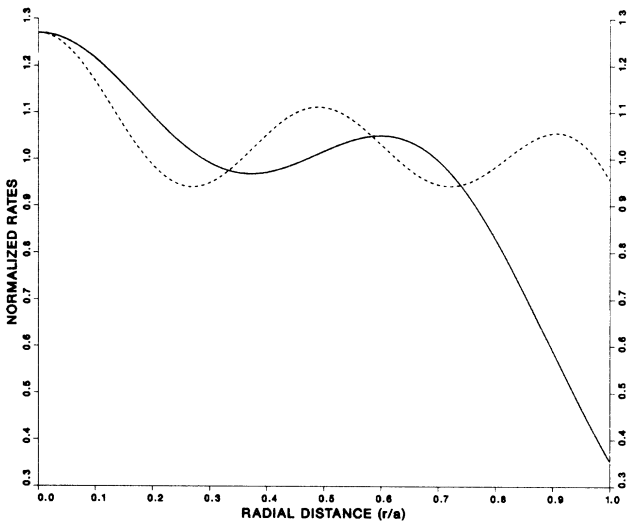

FIG. 1. Normalized rates $R^{\perp}/R^{\perp}_0$ (solid curve) and $R^{\parallel}/R^{\parallel}_0$ (dashed curve) for a glycerol drop ($\epsilon=2.1609$) in air as functions of the radial distance of the atom from the center, for $ka=5$. The corresponding curves (not shown) for a water drop ($\epsilon=1.7689$) have similar oscillating behavior with smaller amplitudes.

$ka=48.769\,35$. The peak value of the radial rate is 900 times the bulk value. Note the difference in the behavior of the rates for the two polarizations as $r\rightarrow a$. Figure 3 shows the rates at a magnetic multipole ($M57$) resonance at $ka=47.548\,35$. Only the tangential rate is enhanced because the radial rate contains only electric multipole

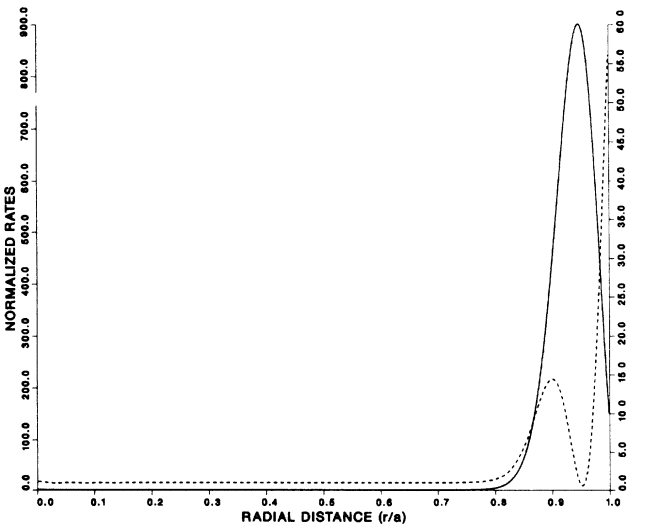

FIG. 2. A large resonance ($E58$) in a water drop ($\epsilon=1.7689$) in air, with $ka=48.769\,356$. The solid curve is the radial rate (scale on the left); the dashed curve is the tangential rate (scale on the right). Both curves oscillate about unity with small amplitudes for $r/a\lesssim 0.8$. The radial rate peaks at $r/a=0.947$.

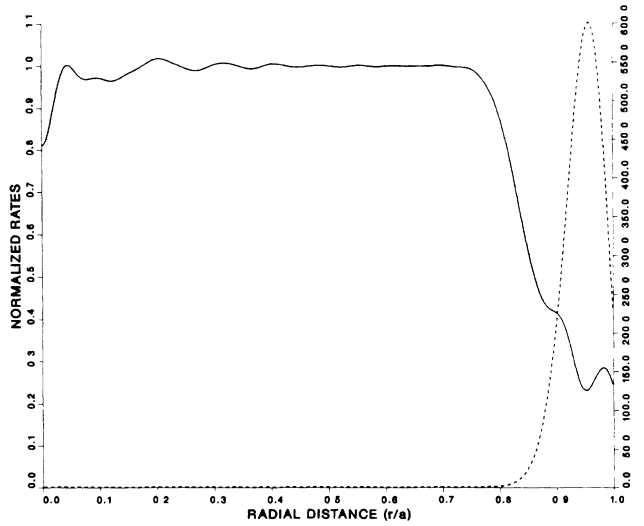

FIG. 3. Another large resonance ($M57$) in a water drop with $ka=47.548\,35$. The tangential rate (dashed curve) peaks at $r/a=0.957$ with a peak value of 601.

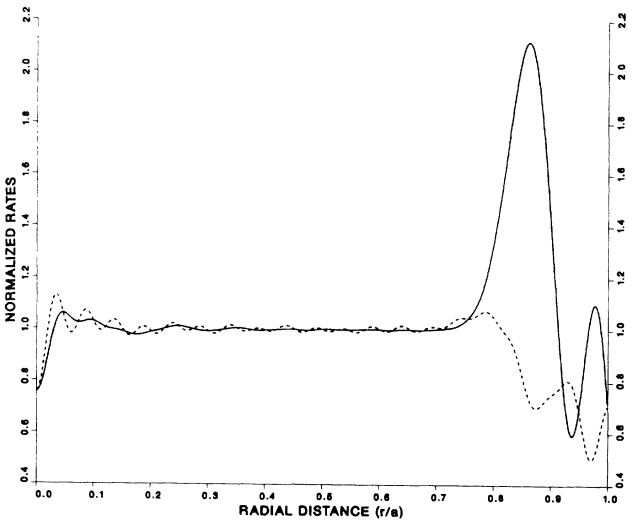

FIG. 5. Effects of a small change in the refractive index on the $M57$ resonance: here $\epsilon=1.7424$ and $ka=47.548\,35$.

terms [see Eq. (1)], while both electric and magnetic multipoles contribute to the tangential rate [see Eq. (2)]. Figures 4 and 5 show how the rates are affected as the physical parameters are varied slightly from their values at the $M57$ resonance. A change of 0.0035% in the size parameter causes the resonance peak in the tangential rate to drop from 600 (Fig. 3) to about 7 (Fig. 4), while a change in the refractive index from 1.33 to 1.32 (a change of 0.75%) causes the resonance to disappear completely (Fig. 5). The next two figures (6 and 7) compare the rates at resonances in larger water drops to the free-space values. Figure 6 shows the large enhancements of the rates (1546 times the free-space value at $r/a=0.848$ for the radial polarization) for $ka=155.068\,598\,6$, when the rates are dominated by a resonance in the $E170$ term. The rates at a nearby magnetic multipole ($M170$) resonance at $ka=154.711\,377$ are shown in Fig. 7. For comparison, the rates under nonresonant conditions ($ka=150$) are shown in Fig. 8, where the rates are normalized to the bulk values (i.e., $1/1.33=0.75$ times the free-space values).

If the radius of the particle is small compared to the wavelength of the transition (the Rayleigh limit), the

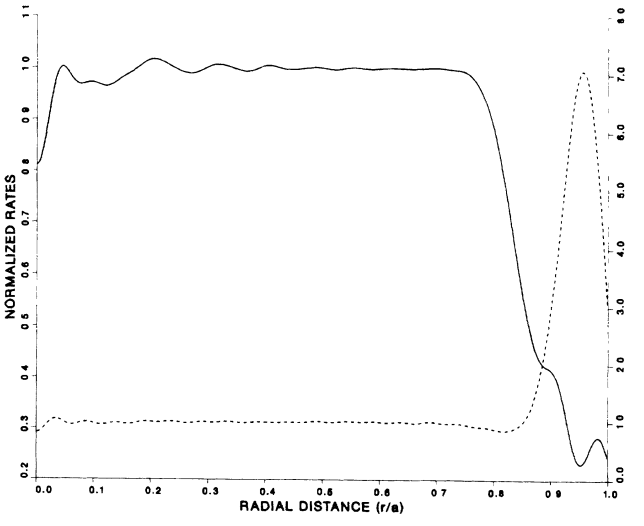

FIG. 4. Effects of a small change in the size parameter on the $M57$ resonance: the rates in a water drop with $ka=47.55$.

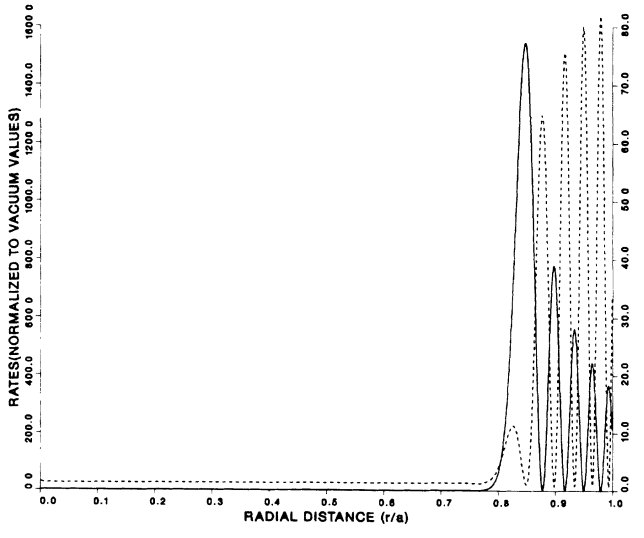

FIG. 6. A sharper resonance ($E170$) in a larger water drop with $ka=155.068\,598\,6$. The radial rate peaks at $r/a=0.848$ with a peak value of 1546 times the free-space value; the tangential rate peaks at $r/a=0.979$ with a peak value of 82.

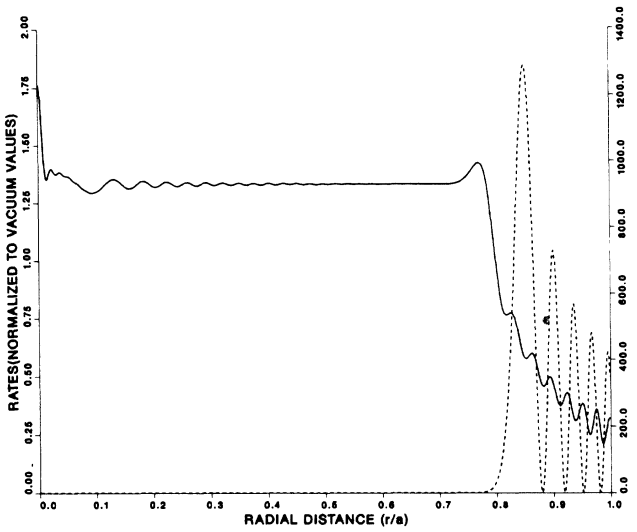

FIG. 7. The $M170$ resonance in a water drop at $ka=154.711\,377$. The tangential rate peaks at $r/a=0.85$, where it is 1287 times the free-space value. Note the difference in the radial dependence of the rates from the electric multipole resonance in Fig. 6.

transition rates are independent of polarization and the location of the atom or molecule within the particle,

$$R/R_0 \rightarrow \frac{9}{(\epsilon_1/\epsilon_2+2)^2}\left[\frac{\epsilon_2\mu_2^3}{\epsilon_1\mu_1^3}\right]^{1/2} \quad \text{for } ka \ll 1 \ . \tag{4}$$

For a nonmagnetic particle in air, this ratio simplifies to $9/[(\epsilon_1+2)^2\sqrt{\epsilon_1}]$. In terms of the free-space rate, we have

$$R/R_{\text{air}}=(R/R_0)(\mu_1^3\epsilon_1/\mu_2^3\epsilon_2)^{1/2} = \frac{9}{(\epsilon_1/\epsilon_2+2)^2}=\frac{9}{(\epsilon_1+2)^2} \tag{4'}$$

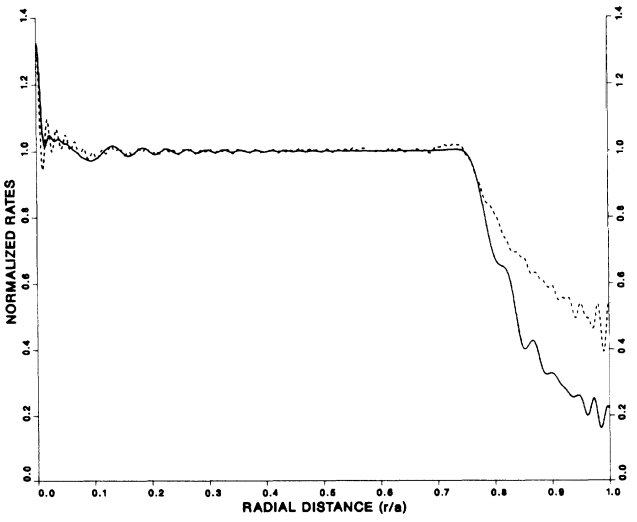

FIG. 8. Normalized rates for a large water drop ($ka=150$) under nonresonant conditions.

(Rayleigh limit). Both ratios (4) and (4') are generally less than unity (as ϵ_1 is ≥ 1 for most dielectrics) and decrease with ϵ_1. These results are readily amenable to experimental test.

III. RADIATION FROM DISTRIBUTION OF ATOMS INSIDE A PARTICLE

Equations (1) and (2) allow us to compute the power radiated by arbitrary distributions of excited atoms inside a dielectric spherical particle, normalized to the power radiated by the same number of atoms in bulk material. The result may be interpreted as the volume average of transition rates of atoms at different sites (and therefore with different lifetimes[11]), and will reflect both the distribution of atoms and the characteristic properties of the particle. Such averages are of physical interest for many reasons. For example, they are relevant in the inverse problem of obtaining information about the distribution of excited atoms and/or the properties of the host particle from the radiation emitted. Another reason is that it is not always feasible to locate atoms at specific sites. In a liquid drop, for example, convection has the effect of washing out inhomogeneities in the distribution. In this section we define average transition rates in the sense mentioned above, and give analytic and numerical results for the special case of a uniform distribution of atoms in a spherical particle, which will sometimes be referred to as a liquid drop for brevity.

Let $n(\mathbf{r})$ be the density of excited atoms inside a spherical dielectric particle. We define the normalized average rate (power) for radial oscillations to be the total (normalized) radiated power for this polarization divided by the total number of excited atoms,

$$\langle R^{\perp}/R_0^{\perp}\rangle=\int (R^{\perp}/R_0^{\perp})n(\mathbf{r}')d^3r' \Big/ \int n(\mathbf{r}')d^3r' \ , \tag{5}$$

where $R^{\perp}/R_0^{\perp}$ is given by Eq. (1) with $y_1=k_1r'$ and the integration is over the particle volume. The average rate $\langle R^{\parallel}/R_0^{\parallel}\rangle$ for tangential oscillations is defined similarly. For a uniform distribution $n(\mathbf{r})=\text{const}$, these averages reduce to

$$\langle R^{\perp}/R_0^{\perp}\rangle=(3/4\pi a^3)\int (R^{\perp}/R_0^{\perp})d^3r' = 2H\sum_{n=1}^{\infty} n(n+1)L_n\,|\,1D_n\,|^2 \ , \tag{1'}$$

$$\langle R^{\parallel}/R_0^{\parallel}\rangle=(3/4\pi a^3)\int (R^{\parallel}/R_0^{\parallel})d^3r' \ , = H\sum_{n=1}^{\infty}\left[\frac{M_n}{|D_n|^2}+\frac{(2n+1)GK_n}{|D_n'|^2}\right] \ , \tag{2'}$$

where

$$G=\mu_1\mu_2/\epsilon_1\epsilon_2 \ ,$$

$$H=(9\epsilon_1/4\rho_1^5)(\mu_1\epsilon_1\epsilon_2/\mu_2)^{1/2} \ ,$$

$$\rho_1=k_1a \ ,$$

and

$$K_n=\int_0^{\rho_1}\rho^2 j_n^2(\rho)d\rho$$
$$=(\rho_1^3/2)[j_n^2(\rho_1)-j_{n+1}(\rho_1)j_{n-1}(\rho_1)]\ , \tag{6a}$$
$$L_n=(2n+1)\int_0^{\rho_1} j_n^2(\rho)d\rho\ , \tag{6b}$$
$$M_n=(2n+1)\int_0^{\rho_1}\{[\rho j_n(\rho)]'\}^2 d\rho\ . \tag{6c}$$

The integrals L_n and M_n may be evaluated by recursion in terms of spherical Bessel functions and the sine integral.[12] However, if one is only interested in the total rate averaged over polarizations,[13] the result is expressible in terms of spherical Bessel functions alone,[12]

$$\langle R/R_0\rangle\equiv\langle R^{\perp}/R_0^{\perp}+2R^{\parallel}/R_0^{\parallel}\rangle/3$$
$$=2H\sum_{n=1}^{\infty}\left[\frac{J_n}{|D_n|^2}+\frac{GK_n}{|D_n'|^2}\right], \tag{7}$$

where

$$J_n=[n(n+1)L_n+M_n]/(2n+1)$$
$$=\int_0^{\rho_1}\{n(n+1)j_n^2(\rho)+[(\rho j_n(\rho))']^2\}d\rho$$
$$=-n\rho_1 j_n^2(\rho_1)+\rho_1^3[j_{n-1}^2(\rho_1)-j_n(\rho_1)j_{n-2}(\rho_1)]/2$$
$$=K_{n-1}-n\rho_1 j_n^2(\rho_1)\ . \tag{8}$$

The persistence of the denominators D_n and D_n' in the average rates (1'), (2'), and (7) shows again the possibility of resonance enhancement of the rates when the transition frequency is near a resonance frequency of the host particle. Figures (9–11) show plots of the normalized average rates as functions of frequency for glycerol ($n=1.47$) and water ($n=1.33$) droplets in air. As in Figs. 1–5 and 8 in Sec. II, the rates have been normalized to the bulk value in medium 1. If they are normalized to the free-space rates, the normalization factor H in Eqs. (1'), (2'), and (7) should be replaced by $9\mu_1^2\epsilon_1^2/(4\rho_1^5\mu_2^2)$ and all the rates in Figs. 9–11 should be multiplied by $\sqrt{\epsilon_1}$. At low frequencies (size parameter $ka\lesssim 10$), the average rates are smooth oscillating functions of ω (Fig. 9), with the peaks getting sharper as the frequency increases. At higher frequencies ($ka\sim 50$), the resonance peaks become huge (Fig. 10). Because the volume integration tends to weigh regions near the surface more heavily than those near the center, a high (low) rate near the surface will generally result in a high (low) average rate as well. For example, the large peak in the radial rate shown in Fig. 2 and in the peak in the average rate at $\lambda=0.901\,842\,9$ μm in Fig. 10 with a peak value of 72 times the bulk rate are both due to the resonance $E57$. The average rate goes through more narrower and closely spaced resonance peaks as ka is increased further (Fig. 11).

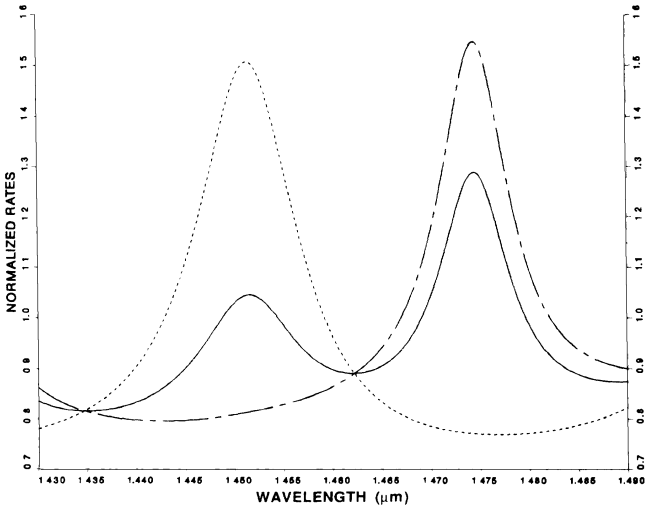

FIG. 9. Normalized rates $\langle R^{\perp}/R_0^{\perp}\rangle$ (dashed curve), $\langle R^{\parallel}/R_0^{\parallel}\rangle$ (long-dashed short-dashed curve), and $\langle R/R_0\rangle$ (solid curve), for a water drop of radius 5 μm. The size parameter ranges from 21 to 22.

IV. SUMMARY AND CONCLUSIONS

We have studied in detail the spatial and frequency dependence of transition rates of single atoms or molecules located in dielectric spherical particles on the basis of a formalism given in Ref. 7. The rates are smooth oscillatory functions of the radial coordinate of the atom at low frequencies, and have huge peaks near the surface at higher frequencies when the transition frequency coincides with a resonance frequency of the host particle. At these resonances the rates are usually dominated by a single resonance term of order slightly larger than the size

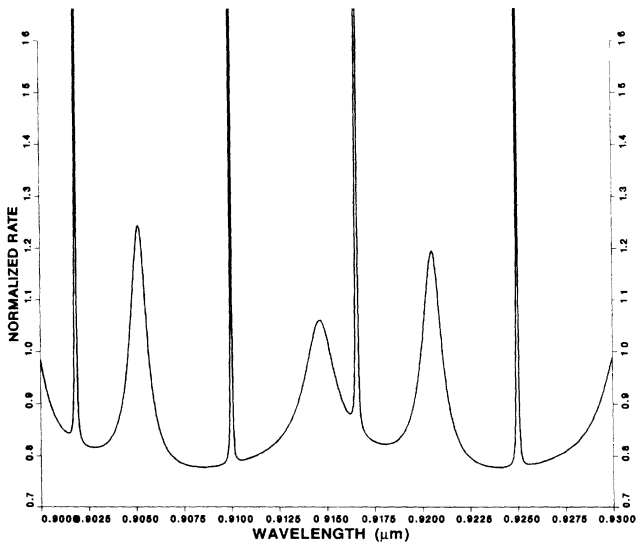

FIG. 10. Frequency dependence of the average total rate $\langle R/R_0\rangle$ for a water drop of radius 7 μm for $ka\sim 50$. The heights and the associated dominating resonances of the four large peaks are, from the left, 72 ($E58$), 108 ($M58$), 60 ($E57$), and 90 ($M57$), respectively. The three small peaks are, from the left, due to resonances in the $M53$, $E52$, and $M52$ terms, respectively.

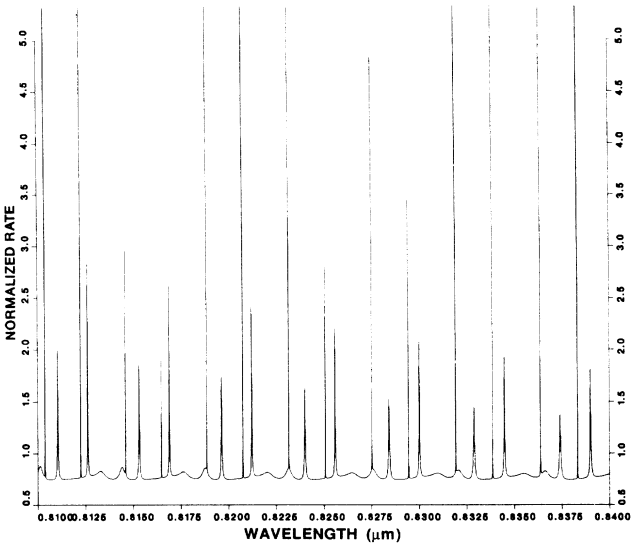

FIG. 11. This plot, with a resolution of $\Delta\lambda=5\times10^{-6}$ μm, shows the qualitative behavior of the frequency dependence of the average rate R/R_0 for a water drop of radius 20 μm. The heights of the narrower peaks are much higher than are shown here. The first ($E170$) and the third ($M170$) peaks from the left have heights of 62.5 (at $\lambda=0.810\,374\,939$ μm) and 99 (at $\lambda=0.812\,246\,06$ μm), respectively. To locate the narrower peaks precisely would have required a resolution of $\Delta\lambda\sim10^{-8}$ μm.

parameter, and can reach values in excess of 1500 times the free-space values at certain locations. Resonances at low values of ka ($\ll50$), as well as resonances of order $\ll ka$ for larger values of ka, do not have such dominant effects in general. The radial dependence of the rates for the two polarizations is quite different for electric and magnetic multipole resonances (see Figs. 2, 3, 6, and 7), because the radial rate contains only electric multipole terms, while the tangential rate contains both electric and magnetic terms [see Eqs. (1) and (2)]. The resonance peaks become higher and narrower as the frequency increases, and are very sensitive functions of the size parameter and the dielectric constant of the particle.

The radiation due to a uniform distribution of excited atoms inside a spherical dielectric particle has been investigated for liquid drops. Explicit expressions are given for the volume-averaged transition rates for both polarizations and for polarization averages. The frequency dependence of the average rates is studied numerically and found to be similar to the behavior of the total scattering cross section of electromagnetic waves by the same particle,[9] viz., smooth oscillatory behavior for low frequencies (Fig. 9), large resonances, for intermediate frequencies (Fig. 10), and a wriggly background with sharp spikes at high frequencies (Fig. 11). The average rate at resonance can be as high as 100 times the bulk rate (or about 130 times the free space rate).

The similarity of the frequency dependence of the rates with that of elastic scattering cross sections can be traced to the fact that the rates are sums of terms corresponding to electric (TM) and magnetic (TE) multipoles [see Eqs. (1), (2), (1′), (2′), and (7)], with denominators D_n and D_n', respectively. These are the same denominators [see Eqs. (3a) and (3b)] as those of the (Mie) scattering coefficients, as well as those of the expansion coefficients of the internal field in the elastic scattering of electromagnetic waves by the same particle.[9] These denominators become small in magnitude at resonant frequencies of the particle, which is the common origin of the resonance in the rates and scattering cross sections, and also of the "hot spots" in spherical particles illuminated by electromagnetic radiation.[10]

When the radius of the particle is small compared to the wavelength of the transition, the transition rate is independent of the position of the atom and is smaller than the rate in bulk medium 1 by a factor

$$9/[(\epsilon_1+2)^2\sqrt{\epsilon_1}]$$

and smaller than the free-space rate by a factor of $9/(\epsilon_1+2)^2$. Experimental tests of these relations as well as our results on the resonance enhancements of the transition rates would be interesting.

We conclude with a brief discussion of some finer points which have not been touched on but which may lead to interesting physical effects. In this paper, the atom is described as a dipole $\mathbf{p}$ oscillating at the (real) transition frequency ω, and the influence of the particle enters primarily through the denominators $D_n(\omega)$ and $D_n'(\omega)$ of Eqs. (3a) and (3b). The enhancements of the transition rates reported here are due to the complex zeros of $D_n(\omega)$ and $D_n'(\omega)$ near the real ω axis, at $\omega=\omega_n=\alpha_n+i\gamma_n$ and $\omega=\omega_n'=\alpha_n'+i\gamma_n'$, respectively, with γ_n and γ_n' small. The imaginary parts γ_n and γ_n' are approximately equal to the widths (or the reciprocals of the lifetimes) of the corresponding multipole resonances.[14] To describe an excited atom, however, the transition frequency ω should actually have an imaginary part γ, which is the reciprocal of the lifetime τ. For our description of spontaneous emission to be valid, it is therefore necessary that $\gamma\ll\gamma_n,\gamma_n'$. Experimentally, the lifetimes of atomic transitions vary over many decades,[15] with $\gamma=1/\tau$ in the range 10^6-10^8 sec^{-1} being common. For comparison, the resonances $M58$ (Fig. 2), $E170$ (Fig. 6), and $M170$ (Fig. 7) discussed in this paper have widths $9.3, 3.2, 2.1\times10^9$ sec^{-1}, respectively. There is thus a broad range of transitions for which our description is valid.[16] When γ becomes comparable with γ_n and γ_n', the decay characteristics become more complicated and other effects,[17] such as oscillatory spontaneous emission, may arise. Also, the frequencies at which large enhancements of the transmission rates occur may deviate significantly from the resonance frequencies of the particle.

In the case of collections of radiating atoms in the a particle, there can be at high atomic densities subtle and interesting collective effects not discussed in Sec. III. These include ringings in the emitted power[18] and superradiance.[19] Detailed treatment of these effects requires more elaborate formalisms than the one employed in this paper. We shall therefore make here only a rough esti-

mate of the critical density of radiating atoms above which collective effects may be expected. Such effects are expected to be small if a photon emitted by an atom has a negligible (i.e., $\ll 1$) probability of being absorbed before it leaves the particle. Consider first the probability p that a photon emitted by one atom will be absorbed by another atom after traveling a distance equal to the average interatomic distance d. Assuming that the direction of emission is random, this probability is roughly $p \approx \sigma/4\pi d^2$, where σ is the photon absorption cross section. This cross section may have values ranging from $\sim 10^{-18}$ cm^2 in nonresonant cases[20] to about λ^2 in resonant cases.[18] The time a photon remains in the particle is approximately $\tau = Q/\omega$, where Q is the mode quality factor. During this time the photon travels a distance[21] $c\tau/n = Qc/n\omega = Q\lambda/2\pi n$, or $(Q\lambda/2\pi nd)$ times the interatomic distance d. The probability P that the photon will be absorbed before leaving the particle is therefore

$$P \approx (Q\lambda/2\pi nd)p = Q\sigma\lambda/8\pi^2 nd^3 .$$

The condition $P \ll 1$ requires that the density $\rho = d^{-3} = 8\pi^2 nP/Q\sigma\lambda$ be much less than the critical density $\rho_c = 8\pi^2 n/Q\sigma\lambda$. As a numerical example, consider the $E170$ resonance shown in Figs. 6 and 11, which has a quality factor $Q \approx 10^6$. For $\lambda \approx 0.8$ μm $= 8 \times 10^{-5}$ cm and $n = 1.33$, we find a critical density $\rho_c \approx 10^{18}$ atoms/cm^3 if $\sigma \approx 10^{-18}$ cm^2, and $\rho_c \approx 2 \times 10^8$ atoms/cm^3 if $\sigma \approx \lambda^2$. For the $E58$ resonance shown in Figs. 2 and 10, Q is around 10^5 and the corresponding critical densities are about ten times as large.

ACKNOWLEDGMENTS

This work was done at the Naval Research Laboratory (NRL). The author would like to thank Dr. A. J. Campillo for interesting discussions and for his kind hospitality at the NRL. The outstanding computing facilities of the NRL are also gratefully acknowledged.

---

*On sabbatical leave from Department of Physics, Clarkson University, Potsdam, NY 13676.

[1]P. Goy, J. M. Raimond, M. Gross, and S. Haroche, Phys. Rev. Lett. **50**, 1903 (1983).

[2]R. G. Hulet, E. S. Hilfer, and D. Kleppner, Phys. Rev. Lett. **55**, 2137 (1985).

[3]D. J. Heinzen, J. J. Childs, J. E. Thomas, and M. S. Feld, Phys. Rev. Lett. **58**, 320 (1987).

[4]K. H. Drexhage, *Progress in Optics,* edited by E. Wolf (North-Holland, Amsterdam, 1974), Vol. 12, p. 165.

[5]R. R. Chance, A. Prock, and R. Silbey, Adv. Chem. Phys. **37**, 1 (1978). This paper contains many references to earlier work.

[6]R. Ruppin, J. Chem. Phys. **76**, 1681 (1982).

[7]H. Chew, J. Chem. Phys. **87**, 1355 (1987). There are several typographical errors in this paper: in Eq. (5), line 2, replace a_E^d by $\bar{a}_E^d(n,m)$, and for $|a_M^d(n,m)\cdots|^2$, read $|a_M^d(n,m)\cdots|^2/k_2^2$; in the line below Eq. (9a), replace $j_n(\rho_2)$ by $j_n(\rho_1)$; in the line below Eq. (9b), add "with index $2 \rightarrow 1$" after (2b); in Table I, for 29 read 290, for 0.88 read 0.94, and for 1.05 read 1.51.

[8]J. M. Wylie and J. E. Sipe, Phys. Rev. A **30**, 1185 (1984).

[9]For expressions of these coefficients for arbitrary media see, for example, the Appendix of H. Chew, P. J. McNulty, and M. Kerker, Phys. Rev. A **13**, 396 (1976). For general discussions of Mie scattering, see, for example, M. Kerker, *The Scattering of Light and Other Electromagnetic Radiation* (Academic, New York, 1969).

[10]See, for example, P. W. Dusel, M. Kerker, and D. D. Cooke, J. Opt. Soc. Am. **69**, 55 (1979); P. Chylek, J. D. Pendleton, and R. G. Pinnick, Appl. Opt. **24**, 3940 (1985); D. S. Benincasa, P. W. Barber, J. Z. Zhang, W. F. Hsieh, and R. K. Chang, *ibid.* **26**, 1348 (1987). The last paper contains additional references.

[11]An exception is the Rayleigh limit, when all the atoms in the particle have the same lifetime (see the last paragraph of Sec. II) and the average rates are equal to the individual rates given by Eqs. (4) and (4'). I would like to thank Dr. A. J. Campillo for discussions on this point.

[12]The details will be given in a separate paper.

[13]The factor of 2 in the first line of Eq. (7) is due to the fact that there are two degrees of freedom associated with the tangential oscillations.

[14]Compare with the Breit-Wigner formula for resonance scattering in quantum mechanics.

[15]W. L. Wiese, M. W. Smith, and B. M. Glennon, *Atomic Transition Probabilities,* Natl. Bur. Stand. Ref. Data Ser., Natl. Bur. Stand. (U.S.) Circ. Nos. 4 and 22 (U.S. GPO, Washington, D.C., 1966), Vol. 1.

[16]The resonances which dominate the transition rates tend to have orders somewhat larger than the value of the size parameter. Because the widths of the resonances decrease with order, the narrow resonances of particles with size parameters much larger than those considered here may lie outside the range of validity of our description for the more common atomic transitions.

[17]For discussions of related electromagnetic phenomena in cavities, see, for example, G. Goubau, *Electromagnetic Waveguides and Cavities* (Pergamon, New York, 1961).

[18]See, for example, H. Walther, in *Quantum Electrodynamics and Quantum Optics,* edited by A. O. Barut (Plenum, New York, 1984).

[19]For discussions of the case of two-level atoms, see, for example, L. Allen and J. H. Everly, *Optical Resonances and Two-Level Atoms* (Wiley, New York, 1975).

[20]See, for example, H. Massey, *Atomic and Molecular Collisions* (Halsted, New York, 1979).

[21]Here n denotes the refractive index of the particle.